Asian Journal of Chemistry; Vol. 25, Supplementary Issue (2013), S17-S21

ASIAN JOURNAL OF CHEMISTRY

www.asianjournalofchemistry.co.in

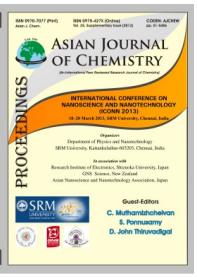

Purification of Single-Wall Carbon Nanotubes by Functionalization and Ultracentrifugation†

E. DIAZ*, C.G. VELAZQUEZ, J. ORTIZ, D. SAUCEDO, G. ORTEGA and A.M. PANIAGUA

ESFM-IPN, Edif. 9 UPALM, Col. San Pedro Zacatenco, Deleg. GAM, México 07738, México

*Corresponding author: Fax: +52 55 55862825; Tel: +52 55 57296139; E-mail: ediazva@gmail.com

AJC-12781

An alternative method is developed for the removal of impurity residuals (metallic nanoparticles, amorphous carbon and fullerenes) resulting from the synthesis of single wall carbon nanotubes (SWNT) by electric arc discharge. For the separation of fullerenes and amorphous carbon, an 'as grown' single wall carbon nanotube sample was subjected to leaching with a Soxhlet apparatus using toluene as solvent. Single wall carbon nanotubes were then functionalized by oxidation for forming carboxylic and hydroxyl groups to increase their solubility for their efficient dispersion with centrifugation. Oxidation was performed with H_2SO_4 and HNO_3 in the presence of potassium persulfate and later they were centrifuged at 23,000 rpm (20,000 g). After these procedures, metallic particles precipitated and the single wall carbon nanotube remained suspended on the water surface from which they were removed by decantation. The purified single wall carbon nanotube sample was characterized by scanning electron microscopy, X-ray diffraction and Raman spectroscopy with results showing evidence of impurity removal with the applied procedures.

Key Words: Single-wall carbon nanotubes, Purification, Functionalization, Ultracentrifugation.

INTRODUCTION

In recent years, the interest and use of carbon nanotubes (CNTs) in the manufacture of optoelectronic and electrochromic devices such as flexible photovoltaic cells[1-3], quantum-well light-emitting diodes[4], flexible electrodes[5], back contacts in solar cells[6], *etc.*, has increased. For these applications, transparent conducting CNT films on flexible substrates are required[7,8]. In order to obtain homogeneous films with high quality CNTs, it is required; above all, a high degree of purified CNT material. Other recent applications involving purification and functionalization of CNTs is their utilization as conducting channels in field effect transistors for biomolecule sensing[9]. If we consider that the commercial cost of pure CNTs is of 50 to 80 dollars per gram, the process of purification and separation of impurities such as fullerenes, amorphous carbon and metallic catalyst mostly determine the entire cost. Single wall carbon nanotubes (SWNT) can be grown by laser ablation[10], chemical vapour deposition (CVD)[11,12], spray pyrolysis[13] and electric arc discharge methods[14,15], among others. Even though with electric arc discharge synthesized SWNTs end up with a considerable amount of impurities, this method is of interest because of the good structural quality of the obtained SWNTs, which is better than the one obtained with CVD growth and is low cost and easier to implement than laser ablation. Then, the problem to be addressed in the preparation of SWNTs by electric arc discharge is to eliminate the impurities resulting from the synthesis process. Many methods of SWNT purification have been developed, such as: hydrothermal[16], to remove amorphous carbon; microfiltration[17], to eliminate metallic nanoparticles; solvent extraction[18], commonly used to remove fullerene particles; acid treatment[19], to dissolve catalytic particles; air oxidation[20], to eliminate amorphous carbon; microwave acid digestion[21], to minimize purification times; high temperature thermal treatments[22], to remove functional groups created during acid treatment, *etc*. In this work, we described a combined process for the purification of mass amounts of SWNTs.

EXPERIMENTAL

A powder mixture composed of 95.25 mol % of graphite (sample A), as carbon source and 2.6 mol % of nickel, 0.7 mol % of iron, 0.7 mol % of cobalt and 0.75 mol % of iron sulfide, as catalysts, were used to prepare a pellet (sample B). This pellet was used as anode and a graphite bar with a sharpened tip was used as cathode.

General procedure: The experimental setup for arc discharge is similar to the one described elsewhere[23]. Briefly,

†International Conference on Nanoscience & Nanotechnology, (ICONN 2013), 18-20 March 2013, SRM University, Kattankulathur, Chennai, India

inside a reaction chamber filled with hydrogen gas at 26664.4 Pa of pressure, applying a DC current of 150 amperes at 30 volts generates an electric arc discharge between the electrodes. The cathode is inclined about 60º with respect to the anode to obtain synthesized material ejected in different directions inside the reaction chamber. Synthesized material was collected from the top, from the wall and from the bottom of the chamber, as well as, in the form of a web like material (samples C, D, E and F, respectively). 300 mg of sample F were refluxed with 80 mL of toluene during 4 h in a Soxhlet extractor and then washed with deionized water and dried (sample G). Part of this sample was diluted in deionized water and subjected to an ultrasonic bath during 0.5 h. This sample was then centrifuged at 23,000 rpm during 1 h. Three samples were obtained as products of this centrifugation: a precipitate, an aqueous solution and a supernatant material which should consist of purified SWNTs. All of these samples were vacuum-filtered using carbolite (carbon 50-0926) membranes with 0.4 μm pore size to obtain samples H, I and J, respectively. These three samples remained supported on the filtering membranes for XRD and Raman analysis. A second procedure was applied to other part of sample F, by subjecting it to reflux with toluene during 8 h in a Soxhlet extractor. After washing with deionized water and drying, 200 mg of this sample was put into reaction with 6 mL of a mixture of H_2S0_4:HNO_3 in a 3:1 volume ratio and 0.5 g of surfactant potassium persulfate in continuous agitation during 15 min for one sample and 4 h for other sample (sample K). This sample was washed with deionized water, ultrasonicated during 45 min and centrifuged during an hour at 23,000 rpm and finally it was vacuum-filtered (sample K). This sample also remained supported on the filtering membrane for XRD and Raman analysis.

Detection method: The described procedures, from catalytic mixture preparation to the last stage of SWNT purification, were followed by X-ray diffraction (XRD) and Raman measurements. X-ray diffraction profiles were obtained in θ/2θ configuration with Cu-K_α radiation, in a D8 focus Bruker AX diffractometer. Raman spectra were obtained in a Horiba Jobin Yvon Raman spectrometer with 785 nm excitation. Micrographs from several SWNT purification stages were obtained with secondary electrons in a Sirion-FEI scanning electron microscope with Everhart-Thornley and TTL detectors.

RESULTS AND DISCUSSION

Fig. 1 shows XRD profiles for 2θ in the range from 10º to 65º for all samples subjected to purification procedures. Crystalline phases are identified as graphitic type (sp^2) carbon as well as metallic catalysts (Ni, Fe, Co).

Fig. 2 presents XRD profiles for 2θ in the range from 5º to 20º for samples B, F, G, H, I, J and K that correspond to: graphitic carbon and catalytic mixture, reaction product, sample purified with toluene reflux, precipitate after centrifugation, aqueous solution after centrifugation, purified SWNTs without functionalizing and functionalized SWNTs, respectively.

Figs. 3 and 4 show Raman spectra for samples subjected to purification procedures.

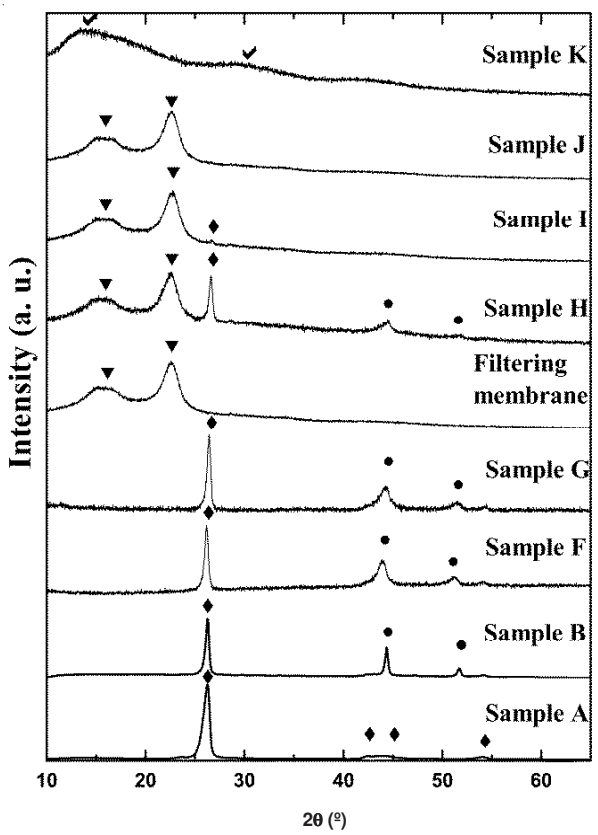

Fig. 1. XRD profiles for 2θ in the range from 10º to 65º for all samples subjected to purification procedures. ■ Graphitic carbon, ● metallic catalysts, ▼ filtering membrane, ✓ possible SWNT signal

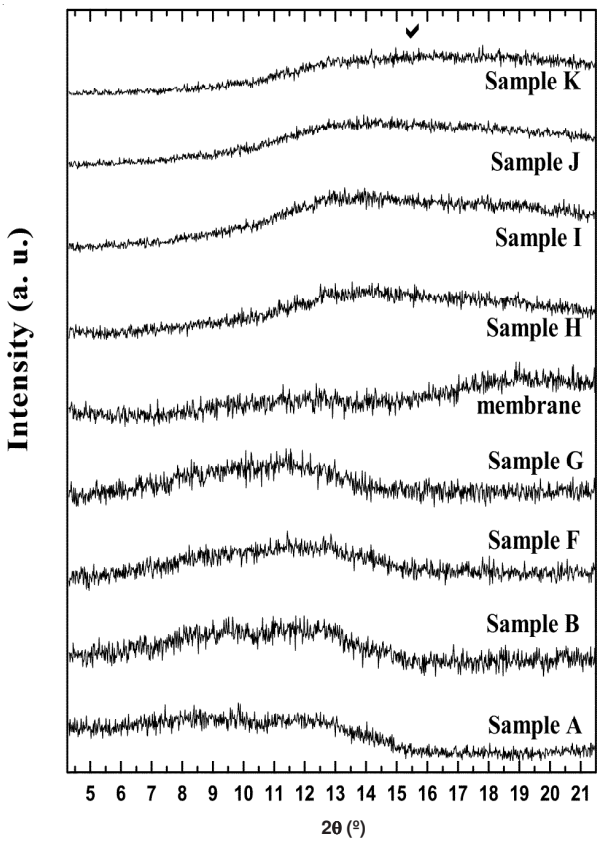

Fig. 2. XRD profiles for 2θ in the range from 2º to 10º for samples subjected to purification procedures. ✓ Possible SWNT signal

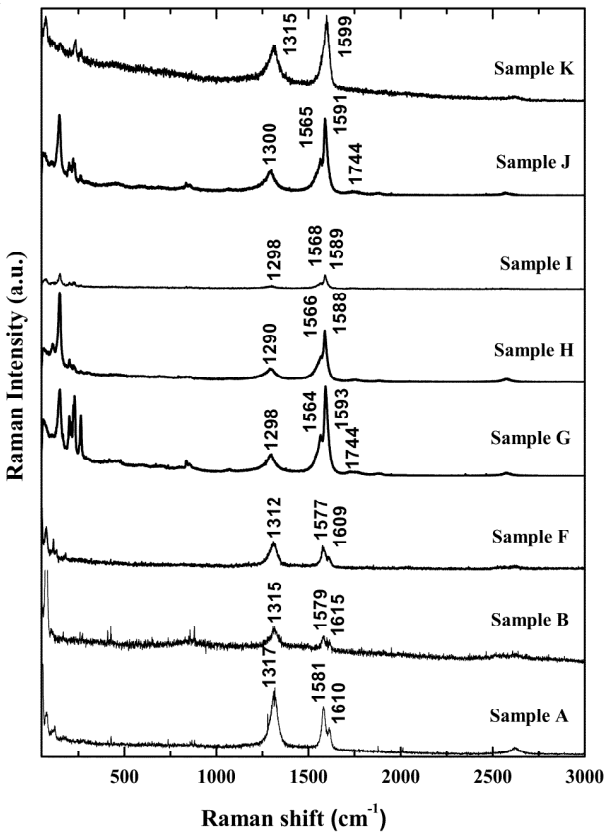

Fig. 3. Raman spectra for all samples subjected to purification procedures

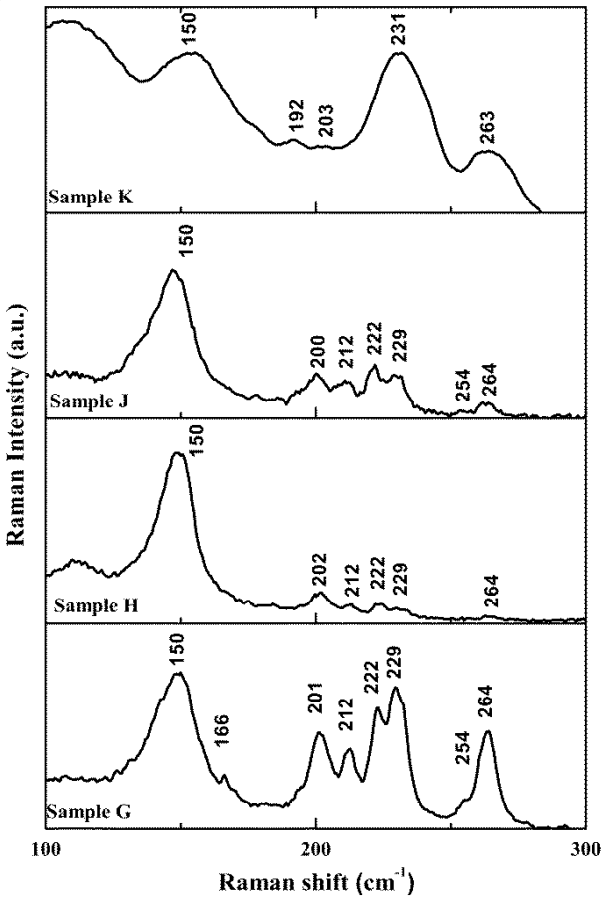

Fig. 4. Raman radial breathing modes of samples in the last stages of purification process

SEM micrographs of reaction product F, of sample G purified with toluene reflux and of functionalized sample K, are shown in Figs. 5-7, respectively.

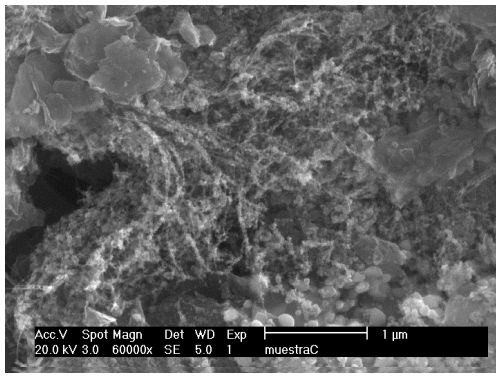

Fig. 5. SEM micrograph of as-grown SWNT.

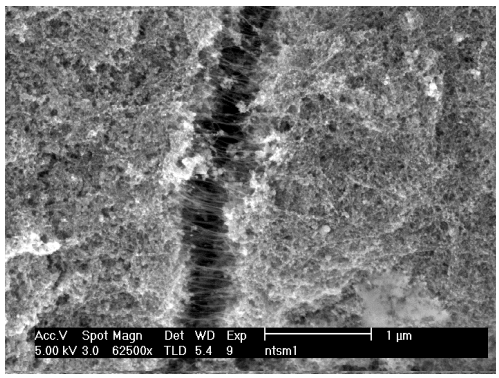

Fig. 6. SEM micrographs of SWNT after toluene reflux

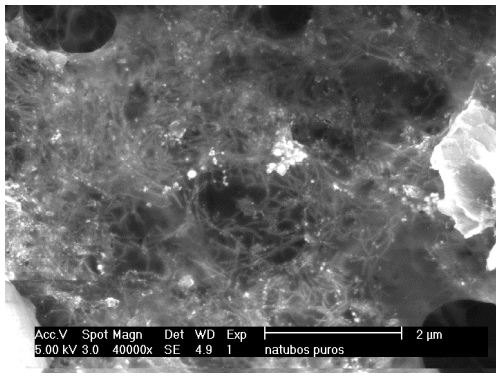

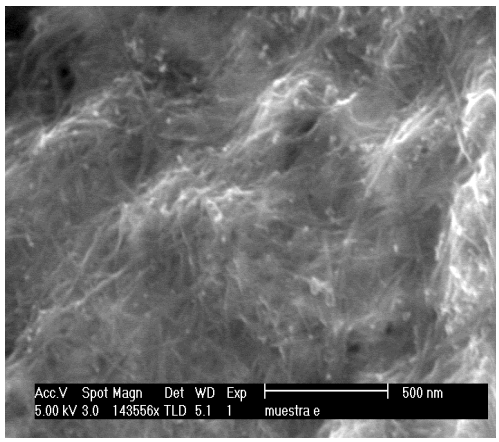

Fig. 7. SEM micrographs of functionalized SWNT after ultracentrifugation for: a) 15 min, b) 4 h

The structural evolution of the purification/functionalization procedures applied to our raw material is shown in Fig. 1 viewed through XRD measurements. The starting graphite powder material of sample A is clearly identified, while the XRD profile of sample B shows the added presence of metallic catalysts in the catalytic powder mixture. After reaction, the XRD profiles of the products C, D, E and F show the presence of carbon and metallic catalysts with different relative quantities depending on where they were collected. XRD profile of sample G, purified with reflux of toluene, shows no marked difference with sample F, in which graphite and metallic catalysts Fe, Ni and Co are identified as well. XRD profiles of centrifugation products show in the precipitate (sample H) presence of graphite and metallic catalysts indicating that ultracentrifugation is a good method to separate them from SWNT. The aqueous solution of sample I shows trace content of graphitic carbon but not of catalysts. The supernatant material containing SWNTs (as observed by SEM), without functionalization (sample J) as well as functionalized (sample K), both show no trace of graphitic carbon or metallic catalysts. These results are in agreement with the ones observed for 2θ in the region between 10° to 60° as reported by Cho *et al.*[15]. Functionalization of SWNT consisted of their oxidation to form carboxylic and hydroxyl groups to make them water soluble in order to separate them easily with centrifugation. XRD profile of sample K does not show the filtering membrane profile, but below 22º in 2θ, a wide band is observed that we attribute to functionalized SWNTs. XRD measurements for 2θ in the range from 4º to 22º (Fig. 2) show the same profile for graphite (sample A), the catalytic mixture (sample B) and the synthesis products C, E and F. It is worth pointing out that in sample G refluxed with toluene the wide band for 2θ between 8º and 14º is slightly more evident. This band disappears in the next stages of purification, but a new wide band for 2θ between 10º and 22º appears in the XRD profile of samples H, I and J. This last contribution becomes wider in the functionalized sample (sample K) and indicates the presence of functionalized SWNTs.

Raman spectroscopy was also employed to follow the changes occurring during synthesis and purification procedures from the raw material to purified samples (Figs. 3 and 4). For SWNT the Raman analysis, two spectral regions are of interest. The first one is related to defect induced (D band) and tangential (G-band) vibrational modes, which are located in the range between 1750 to 1000 cm^{-1}. The second region is related to the radial breathing modes (RBM) and is located from 300 to 100 cm^{-1}. The G band in graphitic carbon is located at about 1582 cm^{-1} but in SWNTs splits into two components above and below this frequency due to the curvature of their structure. The D-band, located around 1350 cm^{-1}, is related to structural and chemical disorder both in graphite and in SWNTs and indicates the presence of amorphous carbon, defective tubes, impurities or SWNT structural perturbation by the incorporation of functionalization groups[24]. In Fig. 3, for graphite (sample A) and catalytic mixture (sample B) both D and G bands are seen at positions around 1315 and 1580 cm^{-1}, respectively. The G band exhibits a shoulder around 1610 cm^{-1}, which is a feature that has been attributed to a weak disorder-induced vibrational feature in graphite and graphene[25], although a weak feature at about the same frequency can also be seen in bundled SWNTs[26]. All these features remain in the collected material after SWNT synthesis (sample F). The weak signal seen at low frequencies for samples A and B can be attributed to graphite nanoparticles, while for sample F it should be related to the presence of SWNTs. After the first stage of purification (reflux with toluene, sample G) the Raman spectra shows the presence of SWNTs characterized by the splitting of the G band into the so called G+ band at 1593 cm^{-1} and G- band at 1564 cm^{-1} due to SWNT wall curvature. The D-band appears around 1298 cm^{-1} with a ratio of band intensities $I_D/I_G = 0.18$, whereas for the centrifuged J-sample and for the functionalized centrifuged K-sample these ratios become 0.25 and 0.61, respectively. These results show diminishing structural quality of SWNTs from the raw synthesized material with the purification process. The Raman signal observed in the low frequency range corresponds to the radial breathing (RBM) modes of SWNTs, which can be used to estimate their diameter[27]. This can be done with the relation $d = 248/\nu$, where d is the SWNT diameter (nm) and ν is the Raman frequency shift (cm^{-1}) of the observed RBM mode[28]. In Fig. 4, RBM bands are shown for purified samples. With the above mentioned equation, SWNT diameters were calculated to be in the range between 0.92 nm and 1.09 nm. The band at 150 cm^{-1} that appears only in the functionalized sample K can be due to SWNT surface modification by functionalization that changes RBM frequencies giving rise to this new band.

By scanning electron microscopy (SEM), the morphological and microstructural changes, from the reaction mixture to the final purified SWNTs, were also followed. The SEM micrographs of the as-grown SWNT presented in Fig. 5 show carbon nanotubes decorated with metallic catalytic particles surrounded by a significant quantity of amorphous carbon and graphite nanoparticles. After leaching with toluene the sample G still presents graphite and amorphous carbon, as well as metallic particles, Fig. 6. The sample without functionalization after centrifugation shows diminishing presence of carbonaceous and metallic nanoparticles. Sample functionalized before ultracentrifugation shows an appreciable decrease of the carbonaceous particles, although metallic nanoparticles are still present (Fig. 7). This last image shows that the purified and functionalized material maintain indeed the tubular SWNT geometry in spite of the strong acid treatment applied.

Conclusion

Purification of SWNT synthesized by electric arc discharge by leaching with toluene and combined with ultracentrifugation showed decrease of carbonaceous impurities, although did not eliminate all the nanometallic particles. DRX, SEM and Raman characterization allow us to follow the structural and morphological changes beginning from raw material to purified and functionalized single-wall carbon nanotubes. The strong acid treatment does not destroy the single-wall carbon nanotubes geometry. Careful studies remain to be done with transmission electron microscopy to observe and characterize structural modifications of single-wall carbon nanotubes by the functionalization method employed in this work.

ACKNOWLEDGEMENTS

The authors gratefully acknowledged financial support to the SIP-IPN projects No. 20120035, 20121703 and to Centro de Nanociencias-IPN for its support in the Raman measurements. Special thanks to Luis Alberto Moreno Ruiz for Raman measurements.

REFERENCES

1. E. Kymakis, E. Stratakis and E. Koudoumas, *Thin Solid Films*, **515**, 8598 (2007).
2. S. Barazzouk, S. Hotchandani, K. Vinodgopal and P.V. Kamat, *J. Phys. Chem. B*, **108**, 17015 (2004).
3. A.J. Miller, R.A. Hatton and S.R. Silva, *Appl. Phys. Lett.*, **89**, 123115 (2006).
4. K. Lee, Z. Wu, Z. Chen, F. Ren, S.J. Pearton and A.G. Rinzler, *Nano Lett.*, **4**, 911 (2004).
5. L. Hu, G. Gruner, D. Li, R.B. Kaner and J. Cech, *J. Appl. Phys.*, **101**, 016102 (2007).
6. T.M. Barnes, X. Wu, J. Zhou, A. Duda, J. van de Lagemaat and T.J. Coutts, C.L. Weeks, D.A. Britz and P. Glatkowski, *Appl. Phys. Lett.*, **90**, 243503 (2007).
7. M.A. Lazar, J.K. Tadvani, W.S. Tung, L. Lopez and W.A. Daoud, *Mater. Sci. Eng.*, **12**, 1 (2010).
8. Y. Zhou, L. Hu and G. Grüner, *Appl. Phys. Lett.*, **88**, 123109 (2006).
9. G. Gruner, *Anal. Bioanal. Chem.*, **384**, 322 (2006).
10. F. Hennrich, S. Lebedkin, S. Malik, J. Tracy, M. Barczewski, H. Rösner and M. Kappes, *Phys. Chem. Chem. Phys.*, **4**, 2273 (2002).
11. D. Selbmann, B. Bendjemil, A. Leonhardt, T. Pichler, C. Täschner and M. Ritschel, *Appl. Phys. A*, **90**, 637 (2008).
12. R. Engel-Herbert, H. Pforte and T. Hesjedal, *Mater. Lett.*, **61**, 2589 (2007).
13. I. Khatri, T. Soga, T. Jimbo, S. Adhikari, H.R. Aryal and M. Umeno, *Diamond Rel. Mater.*, **18**, 319 (2009).
14. S.R.C. Vivekchand and A. Govindaraj, *Proc. Indian Acad. Sci.*, **115**, 509 (2003).
15. H.G. Cho, S.W. Kim, H.J. Lim, C.H. Yun, H.S. Lee and Ch.R. Park, *Carbon*, **47**, 3544 (2009).
16. K. Tohji, H. Takahashi, Y. Shinoda, N. Shimizu, B. Jeyadevan, I. Matsuoka, Y. Saito, A. Kasuya, S. Ito and Y. Nishina, *J. Phys. Chem. B*, **101**, 1974 (1997).
17. S. Bandow, A.M. Rao, K.A. Williams, A. Thess, R.E. Smalley and P.C. Eklund, *J. Phys. Chem. B*, **101**, 8839 (1997).
18. C.M. Schauerman, J. Alvarenga, B.J. Landi, C.D. Cress and R.P. Raffaelle, *Carbon*, **47**, 2431 (2009).
19. X. Zhao, M. Ohkohchi, S. Inoue, T. Suzuki, T. Kadoya and Y. Ando, *Diamond Rel. Mater.*, **15**, 1098 (2006).
20. K. Tohji, T. Goto, H. Takahashi, Y. Shinoda, N. Shimizu, B. Jeyadevan, I. Matsuoka, Y. Saito, A. Kasuya, T. Ohsuna, K. Hiraga and Y. Nishina, *Nature*, **383**, 679 (1996).
21. H. Li, L. Feng, L. Guan, Z. Shi and Z. Gu, *Solid State Commun.*, **132**, 219 (2004).
22. A.C. Dillon, T. Gennett, K.M. Jones, J.L. Alleman and M.J. Heben, *Adv. Mater.*, **11**, 1354 (1999).
23. V. Cruz-Alvarez, J. Ortiz-López, C. Mejía-García, J.S. Arellano-Peraza, V.M. Sánchez-Martínez and J. Chávez-Carvayar, *Fullerenes, Nanotubes Carbon Nanostruc.*, **13**, 299 (2005).
24. V. Tzitzios, V. Georgakilas, E. Oikonomou, M. Karakassides and D. Petridis, *Carbon*, **44**, 848 (2006).
25. L.M. Malard, M.A. Pimenta, G. Dresselhaus and M.S. Dresselhaus, *Physics Reports*, **473**, 51 (2009).
26. M.S. Dresselhaus, G. Dresselhaus and A. Jorio, *Ann. Rev. Mater. Res.*, **34**, 247 (2004).
27. A. Jorio, R. Saito, J.H. Hafner, C.M. Lieber, M. Hunter, T. McClure, G. Dresselhaus and M.S. Dresselhaus, *Phys. Rev. Lett.*, **86**, 1118 (2001).
28. R. Saito, G. Dresselhaus and M.S. Dresselhaus, *Phys. Rev. B*, **61**, 2981 (2000).